Published in final edited form as:
Dev Biol. 2013 September 1; 381(1): 107–120. doi:10.1016/j.ydbio.2013.06.007.

Regulation of pre-natal circle of Willis assembly by vascular smooth muscle Notch signaling

Ke Yang[1], **Suhanti Banerjee**[1], and **Aaron Proweller**[1,*]

[1]Case Cardiovascular Research Institute and University Hospitals Harrington Heart and Vascular Institute, Case Western Reserve University School of Medicine, Cleveland, Ohio 44106

Abstract

The circle of Willis (cW) is a major arterial collateral structure interconnecting hemispheric circulation within the brain, and in humans, anatomical variation of the cW is linked to stroke risk. Our prior studies in adult mice deficient in vascular smooth muscle cell (vSMC) Notch signaling revealed altered cerebroarterial maturation and patterning, including an anatomically incompetent cW similar to human variants. However, a developmental dependency on Notch signaling for cW formation in this model remained uncharacterized. Through temporospatial embryonic analyses, we now demonstrate that cW assembly is a pre-natal process highly sensitive to vSMC Notch signals, whose absence results in delayed nascent vascular plexus formation and under-development of the cW including the key anterior communicating artery (AComA) interconnecting anterior forebrain circulation. Mutant embryos additionally feature reduced vSMC coverage, non-uniform calibers and asymmetric branching at bifurcations of the major proximal cerebral arteries. At the cellular level, a notable reduction in vascular endothelial cell proliferation exists in the region of AComA assembly despite the presence of Vegfa. Furthermore, Notch signaling-deficient vSMCs in developing cerebral vessels feature reduced Pdgfrβ and Jagged1 levels and impaired proliferation. These collective findings in the embryonic brain support studies in adult animals demonstrating a reliance on intact vSMC Notch signaling for optimal neovascular responses to angiogenic stimuli. Importantly, the new data provide unique insights into the native formation of the cW and underscore a pioneering developmental role for vSMC Notch signaling in regulating temporospatial assembly of the clinically relevant cW.

Keywords

Notch signaling; angiogenesis; vascular smooth muscle cell; circle of Willis

Introduction

Developmental angiogenesis features both common and tissue-specific molecular pathways supporting distinct organizational and functional requirements of the end-organ. Coalescence of endothelial cell (EC) precursors results in tubular networks through a process termed vasculogenesis. Subsequent “angiogenic” remodeling featuring EC

Corresponding author: Aaron Proweller, MD, PhD, Case Western Reserve University, Department of Medicine, University Hospitals Harrington Heart and Vascular Institute, and The Case Cardiovascular Research Institute. 4530 Wolstein Research Building 2103 Cornell Road, Cleveland, OH 44106, Tel: 216-368-0131, Fax: 215-368-0556, aaron.proweller@case.edu.

proliferation, sprouting, branching and regression overlaps with “vascular myogenesis” characterized by the participation of vSMCs and pericytes (PC) providing structural and functional support for assembly of competent blood vessels. Cell lineage studies examining early patterns of mammalian embryonic CNS vascularization suggest that cerebrovascular PCs/vSMCs originate primarily from cephalic neural crest in branchial arch assembly in contrast to mesodermal derivatives in the trunk and limb regions (Etchevers et al., 2001; Korn et al., 2002; Majesky, 2007). Though neural crest-derived PC/vSMCs influence blood flow, microvessel stabilization and blood-brain-barrier integrity, much less is understood of the coordinate cellular and molecular signals in vSMCs required for successful regional developmental of cerebral arteries and in particular, the circle of Willis (cW) (Armulik et al., 2010; Bonkowski et al., 2011).

In the cerebral circulation, the cW is a prominent arterial collateral structure interconnecting anterior hemispheric and posterior forebrain circulation and provides autoregulatory blood flow support during dynamic changes in systemic blood pressure and intravascular volume. Large variations in cW organization exist among mammalian species, and in humans, suboptimal cW formation is a risk factor for ischemia and stroke in the setting of occlusive carotid artery disease (Barone et al., 1993; Hoksbergen et al., 2003; Profice et al., 2011). In contrast to the human cW with a normally preserved anterior communicating artery (AComA) and posterior communicating arteries (PComA, linking anterior and posterior cerebral circulation), the cW in mice typically lacks PComAs thereby rendering two discrete vascular distributions: the internal carotid artery (ICA)/anterior and basilar artery (BA)/posterior domains (Okuyama et al., 2004; Proweller et al., 2007). Therefore, mice largely rely on the critical AComA to maintain inter-hemispheric tissue perfusion within the anterior cerebrum.

Knowledge of the cellular and molecular influences that guide cW assembly or of the timing required for its maturation is incomplete. We previously described an adult mouse model (SM22-Cre^{+}/DNMAML1^{+}) deficient in vSMC Notch signaling featuring abnormal cW connectivity that was neurologically incompatible with induced unilateral ICA occlusion, a scenario that recapitulates symptomatic unilateral ICA disease in humans with incomplete (variant) cW anatomy (Proweller et al., 2007). This study particularly demonstrated the importance of an intact cW AComA segment for maintenence of inter-hemispheric tissue perfusion within the anterior cerebrum in the setting of ICA occlusion. However, the precise contributory role(s) for vSMC Notch signaling during presumptive embryonic development of the cW in this animal model remained unexplored. Therefore, we hypothesized that abnormal cW anatomy observed in the adult mice could be explained by a gestational requirement for Notch signaling in cerebral vSMCs conferring optimal cell function.

As such, we have undertaken a precise developmental mapping of cW formation to delineate the interdependency between cerebral vSMC Notch signaling and proper cW assembly. Utilizing SM22-Cre^{+}/DNMAML1^{+} mice, we define and contrast the temporospatial development of the cW in littermate control and Notch signaling-deficient embryos. We highlight the formation of the key AComA and characterize the behavior of vascular wall cells in this process. Together, our findings demonstrate a regional dependence of vSMC Notch signals on cell function and prenatal cW formation, and we discuss these results in view of our prior studies in adult animals wherein vSMC Notch signaling provides instructive cues to neighboring ECs important for optimal angiogenesis (Yang and Proweller, 2011).

Materials and methods

Animals

The generation and initial characterization of SM22-Cre$^+$/DNMAML1$^+$ (DNMAML1-expressing) and littermate control SM22-Cre$^-$/DNMAML1$^+$ (non-DNMAML1-expressing) mice (including the down-regulation of Notch signals and target genes in vSMC cells from SM22-Cre$^+$/DNMAML1$^+$ animals) were reported previously (Proweller et al., 2007). All mice, including parental lines SM22-Cre$^+$ and conditional DNMAML1, were maintained in a C57BL/6 genetic background. Animal experimentation was performed under approved protocols from the Case Western Reserve University Animal Care and Use Committee and National Institutes of Health guidelines.

μ-CT vascular imaging and sample preparation

Embryonic day (E)11.5 to 15.5 embryos were perfused with a solution containing 50-200 μl of BaSO4 compound (30%), heparin (25 U/ml) and gelatin (2.5%) by transmyocardial injection. Intravascular filling was allowed to solidify for 30 min on ice followed by 4% paraformaldehyde fixation. Perfused embryos were scanned on a GE Preclinical eXplore Locus Micro CT (GE Healthcare, Chalfont St. Giles, U.K.). Images were acquired using X-ray tube voltage of 80 kV with a tube current of 500 μA. The exposure time utilized was 2 sec. The detector bin was set to 1×1, providing a full resolution of 20 μm. Images were acquired every degree of rotation, creating 360 raw data projections. These projections were corrected, unwrapped and reconstructed using GE's proprietary reconstruction algorithms to create a full 3-dimensional reconstruction of the scanned specimen.

Whole mount immunostaining

E11.5-15.5 embryos were harvested and perfused transmyocardially with 5-20 μl Dylight 594-lectin (Dako), fixed with 4% paraformaldehyde for 1 hr at room temperature (or 16 hr at 4 °C) and washed in PBS. Lectin-labeled brain tissues were carefully dissected for whole mount staining with FITC-conjugated mouse anti-SMA antibody (Sigma) followed by imaging using a high-resolution inverted fluorescence microscope (Leica DMI6000B).

Immunohistochemistry

Embryonic brains were fixed in 4% PFA for 1 hr at room temperature followed by overnight incubation in 30% sucrose. Immunohistochemistry was performed on 10 μm thick transverse or coronal sections from OCT-embedded brains using the following primary antibodies: FITC-conjugated mouse anti-SMA (Sigma), Cy3-conjugated mouse monoclonal anti-smooth muscle α-actin (SMA) 1A4 (Sigma), rabbit polyclonal antibody against NG2 (Millipore) or Pdgfrβ (Cell Signaling), anti-green fluorescent protein (GFP) (Invitrogen), anti-cleaved Caspase 3 (Cell Signaling), anti-Jaggedl, anti-Notch1 and anti-Notch3 (Santa Cruz). Secondary antibodies included Alexa Fluor® 594 or Alexa Fluor® 488 anti-rabbit IgG (Molecular Probes). A complete description of each antibody (including dilutions) and lectin used in this study can be found in Supplemental Table 1.

Cell proliferation and apoptosis measurements

Cell proliferation was assessed by anti-Ki67 immunohistochemistry on transverse or coronal sections from embryonic brains. Ki67 and lectin double-positive cells or Ki67 and SMA double-positive cells in vessels were quantified. For apoptotic measurements, anti-Caspase 3 antibody was used for immunohistochemistry on adjacent sections. Fluorescent images were acquired using a cooled-CCD camera and QCapture 6.0 imaging software (Universal Imaging; Downington, PA).

Statistical analysis

Data are presented as mean±SEM. Statistical analyses were performed using a paired one-tailed Student's t-test. Values of $P<0.05$ were considered significant.

Results

Temporospatial patterning and anomalies of the cW in SM22-Cre$^+$/DNMAML1$^+$ embryos

We embarked on a focused characterization of SM22-Cre$^+$/DNMAML1$^+$ embryos to uncover a developmental contribution of vSMC Notch signaling in cW patterning. This mouse line expresses the pan-Notch inhibitor, Dominant Negative Mastermind-Like 1 (DNMAML1) as an EGFP fusion protein in a SMC lineage-restricted fashion to repress canonical Notch signaling (Proweller et al., 2007). First, expression of DNMAML1 in cerebral arterial smooth muscle was confirmed by anti-GFP immunostaining of E13.5 embryos pre-labeled with lectin for visualization of EC-lined vasculature (Supplemental Fig. 1A-D). As expected, DNMAML1 (GFP) co-localized with expression of smooth muscle cell markers SMA and NG2 in the middle cerebral artery (MCA) from SM22-Cre$^+$/DNMAML1$^+$ embryos but was undetectable in controls (Supplemental Fig. 1E-H, arrowheads in F and H).

Next we determined the temporospatial patterning of the cW and proximal cerebral artery formation in control and SM22-Cre$^+$/DNMAML1$^+$ embryos whose size and intracranial neuronal content and organization were indistiguishable between groups (data not shown). We particularly focused on the developmental formation of AComA, the vital interconnecting arterial collateral of the cW, which we reported absent or attenuated in adult SM22-Cre$^+$/DNMAML1$^+$ animals (Proweller et al., 2007). High-resolution μ-CT imaging and fluorescence angiography/immunostaining were employed in a complementary manner to visualize the developing cerebral arterial segments. From the ventral view of E13.5 control forebrains, μCT imaging identified the proximal vertebral and internal carotid arteries as well as component segments of the cW (Fig. 1A, labeled structures). Of note, the patterning of proximal cerebral arteries (ACA, MCA, PCA, and ICA) is typically complete by E11.5, preceding the appearance of the AComA (data not shown). The overall configuration of the ICAs and BAs of SM22-Cre$^+$/DNMAML1$^+$ embryos was comparable to littermate controls with respect to caliber uniformity and vessel symmetry (Fig. 1A, B). Within the posterior portion of the cW, a PComA connection to the vertebral-basilar circulation was not identified in control embryos, consistent with the known absence or hypoplastic PComA in mice (Okuyama et al., 2004). In E13.5 control embryos, AComA segments were well-visualized (Fig. 1A, red arrowhead). In contrast, there was a notable absence of opacification in the corresponding segment from SM22-Cre$^+$/DNMAML1$^+$ embryos (Fig. 1B, red arrowhead), a finding consistent with interrupted blood filling and an immature plexus observed under bright field imaging (Fig. 1C, E vs D, F, red arrowheads). Additional immunostaining of E13.5 embryos revealed that, in contrast to the well-organized lectin-labeled EC plexus at the AComA site in controls (Fig. 2A, G and M), the mutant plexus appeared immature and malformed (Fig. 2D, J and P). By E1 7.5, control embryos displayed the complete anastomosis of the AComA extending from bilateral ACAs and a symmetric arterial collateral network including the OAs extending from ACAs (Fig. 3C, I and O, arrow). In contrast, AComA formation in E17.5 SM22-Cre$^+$/DNMAML1$^+$ embryos remained compromised (Fig. 3F, L and R, arrow) with notable abnormalities including asymmetric bifurcating branches from the ACA and segmental dilatation of ACAs and OAs (Fig. 3L). Therefore, from these anatomical studies, we conclude that AComA formation in mice is a prenatal process dependent on vSMC Notch signaling.

Impaired vascular smooth muscle coverage in SM22-Cre^{+}/DNMAML1^{+} embryos

To dissect the cellular influences underlying malformation of AComA, ACAs and OAs in SM22-Cre^{+}/DNMAML1^{+} embryos, we assessed the spatial organization of vSMCs associated with cW segments. Lectin-perfused embryos were dissected and whole mount co-stained with anti-SMA antibody to identify vSMC coverage of the cW arterial segments. E13.5 control embryos exhibited extensive SMC coverage and vascular remodeling (Fig. 2B, H-I, N-O) whereas a notable reduction in cW SMC content was apparent in SM22-Cre^{+}/DNMAML1^{+} embryos (Fig. 2E, K-L, and Q-R), resulting in an unremodeled vascular plexus (Fig. 2P-R). By E17.5, control embryos displayed a complete AComA with uniform caliber and vSMC coverage as well as extensive vSMC coverage of MCA and OA conduits (Fig. 3C, I and O, arrowheads). In contrast, SM22-Cre^{+}/DNMAML1^{+} embryos exhibited diminished vSMC content in the region of AComA assembly (Fig. 3F, L and R, arrowheads). Moreover, there were few vSMCs present at branch points of mutant ACAs (Fig. 4D-F and J-L, arrow) in contrast to the vSMC investment observed at these sites in control embryos (Fig. 4A-C and G-I, arrow). Finally, mutant OAs additionally lacked perimural coating and displayed dilated vessel calibers compared to control arteries (Fig. 4L vs I, brackets).

Reduced proliferation of ACA-associated ECs and SMCs in SM22-Cre^{+}/DNMAML1^{+} embryos

We previously demonstrated impaired postnatal angiogenic responses to growth factor (including Vegfa) stimulation in adult SM22-Cre^{+}/DNMAML1^{+} mice and suggested an underlying failure of heterotypic cell signaling from vSMCs to adjacent ECs concomitant with defective SMC migration and proliferation (Yang and Proweller, 2011). Therefore, we hypothesized that poor EC plexus maturation in mutant AComA formation may be a manifestation of a blunted sprouting capacity of ECs from mutant ACA towards available angiogenic cues.

Vegfa/Vegfr-2 signaling is a well-established pathway regulating both physiological and pathological angiogenesis as well as neurovascular development and remodeling (Bauer et al., 1992; James et al., 2009; Vasudevan and Bhide, 2008). We surveyed Vegfa expression patterns in control SM22-Cre^{-}/DNMAML1^{+} brain from stages E11.5 through E15.5. Coronal sections encompassing the developing AComA region were immunostained with Vegfa antibody and lectin or SMA antibody to demonstrate the pattern of Vegfa expression and its temporospatial relationship to vascular structures. At E1 1.5, Vegfa was observed concentrated at the edge of the neural tube in control embryos in a pattern indistinguishable from SM22-Cre^{+}/DNMAML1^{+} embryos (Fig. 5A, B, arrowheads, and data not shown). At the anterior and ventral portion of the developing frontal lobe at E13.5, the AComA plexus was visualized by lectin-labeled ECs in a region associated with intense Vegfa expression consistent with neuronal origin (Fig. 5C, D, arrowheads). By E15.5, the merging and near complete formation of the AComA into a single lumen conduit occurs juxtaposed to a persistent Vegfa gradient (Fig. 5E, F, arrowheads).

Therefore, given the presence of localized Vegfa expression, we ascertained in SM22-Cre^{+}/DNMAML1^{+} embryos whether altered EC and or vSMC proliferation or survival were features of failed arterial maturation of AComA. Proliferative EC and vSMC indices were assessed by Ki67 antigen detection and co-staining with either lectin or SMA, respectively, from E13.5 and E15.5 brain tissues. In representative sections containing the developing AComA, significantly more Ki67/lectin double-positive cells were identified in control versus SM22-Cre^{+}/DNMAML1^{+} tissues (Fig. 6A-E, arrows). Interestingly, proliferation of vascular ECs from non-AComA brain regions did not differ between groups at stages E9.5-E15.5 (Supplemental Fig. 2). Moreover, fewer Ki67/SMA double-positive cells were

consistently measured within SM22-Cre$^+$/DNMAML1$^+$ AComA regions (Fig. 6F-J, arrows). By E15.5, vSMCs associated with neighboring OA and MCA vessels in SM22-Cre$^+$/DNMAML1$^+$ embryos also displayed a statistically significant reduction in proliferative activity (Fig. 7A-L, especially I vs J, and K vs L, and quantitation in M).

Since Notch signaling has been linked to survival of adult vSMCs (Morrow et al., 2009), we further assessed in SM22-Cre$^+$/DNMAML1$^+$ embryos the possibility of AComA regression due to cellular apoptosis. Immunodetection of the apoptotic marker cleaved caspase 3 did not co-localize with SMA-positive vSMCs, suggesting the absence of apoptosis at the region of AComA assembly in E11.5-15.5 embryos (Supplemental Fig. 3). Of note, a few cleaved caspase 3-positive non-vascular cells were detected in the telencephalon region of both control and mutant (E11.5 and E13.5) embryos (Supplemental Fig. 3A, B and E, F, arrowheads), a feature of neural progenitor cell death previously described (Mason et al., 2006). Taken together, these data implicate impaired replicative behavior of both ECs and vSMCs contributing to failed AComA assembly in SM22-Cre$^+$ /DNMAML1$^+$ embryos without evidence for apoptotic-mediated vessel regression.

Diminished PdgfrP and Jagged1 expression in SM22-Cre$^+$/DNMAML1$^+$ cerebral vSMCs

Pdgf (PdgfBB)-Pdgfrβ signaling is, in part, responsible for SMC recruitment during angiogenesis, and Pdgfrβ is directly regulated by Notch signaling (Jin et al., 2008). We have previously reported that aortic SMCs from adult SM22-Cre$^+$/DNMAML1$^+$ mice display reduced PdgfrP expression contributing to abnormal migration in the context of postnatal angiogenesis (Yang and Proweller, 2011). Therefore, we assessed whether a reduction in Pdgfrβ expression is also a feature of developmental cerebral vSMCs, possibly contributing to the mural cell coverage defect observed during prenatal cW assembly. In E13.5 control embryos, AComA/ACA union features conduits enriched in Pdgfrβ$^+$/GFP$^-$ SMCs (Fig. 8A, C, E and G). In contrast, SM22-Cre$^+$/DNMAML1$^+$ embryos typically displayed diminished Pdgfrβ expression within available DNMAML1$^+$ (GFP$^+$) SMCs (Fig. 8B, D, F and H).

Multiple Notch ligands and receptors are expressed in conduit segments (AComA/ACA) including Notch1, Notch3, Jagged1, and Dll4, underlying the importance of the signaling pathway during cerebral cW formation (Supplemental Fig. 4). Furthermore, Jagged1 ligand, known to stimulate angiogenic activity of ECs through engagement with EC Notch receptors (Benedito et al., 2009), is a direct gene target of Notch signaling activation and its expression is down-regulated in adult aortic SMCs from SM22-Cre$^+$/DNMAML1$^+$ mice (Yang and Proweller, 2011). Therefore, we further assessed the arterial expression of Jagged1 in SM22-Cre$^+$/DNMAML1$^+$ embryos during cW assembly at mid-gestation. In control embryos, Jagged1 was consistently detected in vSMCs associated with the AComA/ACA conduit (Fig. 9A, C, E and G); however, in mutant embryos, the ligand was poorly expressed in existing DNMAML1$^+$ (GFP$^+$) vSMCs (Fig. 9B, D, F and H).

Discussion

Cerebral arterial patterning is highly stereotyped, involving several coordinate processes including angiogenesis and arteriogenesis (Mancuso et al., 2008). Temporally and spatially regulated EC-SMC interactions are required for proper vessel assembly and function in cerebral vascularization (Kurz, 2009; Lackovic et al., 2005), yet knowledge of the specific molecular factors controlling regional cerebral vascular patterning *in utero* is incomplete. In the current study, analyses were undertaken to delineate a developmental basis of the cW defects identified in adult SM22-Cre$^+$/DNMAML1$^+$ mice and therefore to better characterize vSMC Notch signaling-dependent mechanisms operating during gestation that presumptively give rise to the variant adult phenotype. Such information would importantly

enhance our understanding of cW assembly in the context of clinically relevant anatomical variants.

Temporospatial AComA assembly is a distinct developmental process

We determined that SMC remodeling or vascular myogenesis of the major proximal cerebral arteries including BAs, VAs, MCAs and ACAs is well-established by E11.5, but the cW (and AComA) for interconnecting the circulation of the anterior hemispheres is not yet formed, consistent with a previous report (Hiruma et al., 2002). Our developmental analyses in control embryos suggested that branching angiogenesis from left and right ACAs forms an initial EC plexus by E12.5 or E13.5 from which the AComA segment arises. However, SM22-Cre^{+}/DNMAML1^{+} embryos exhibited delayed nascent vascular plexus formation and failure of AComA maturation coincident with poor vSMC association. Hence, the cW derangements observed in adult SM22-Cre^{+}/DNMAML1^{+} mice likely reflect disrupted developmental angiogenesis beginning in mid-gestation.

Relationship of regional Vegf gradients and AComA assembly

Many developmental processes including neurovascular patterning are regulated by growth factor gradients. Chemokines such as Vegfa are required for cerebral vascular patterning including early BA formation and pial vascular collateralization in late stage embryos and neonates (Chalothorn and Faber, 2010; Fujita et al., 2011). We identified a localized pattern of Vegfa expression within the neuronal tissue surrounding the key region of AComA assembly in both control and SM22-Cre^{+}/DNMAML1^{+} embryos. This observation suggested that a Vegfa gradient in the growing forebrain may be exquisitely important for AComA plexus formation through angiogenic sprouting from existing ACAs. Moreover, Vegfa is critical for EC survival in the EC plexus (Gerber et al., 1998), yet we did not detect vascular cell apoptotic activity in the AComA region of SM22-Cre^{+}/DNMAML1^{+} embryos. Thus, the impact of reduced Notch signaling in vSMCs with resultant loss of SMC coverage is linked to diminished angiogenic sprouting despite local Vegfa availability.

Notch signaling regulates functional behavior of developmental cerebral vSMCs

Vascular remodeling requires proper SMC differentiation, proliferation, and migration, principally governed by the Pdgf/Pdgfrβ signaling axis. Consistent with our previous findings, Pdgfrβ content is reduced in cerebral vSMCs, confirming its targeted regulation by Notch signaling (Jin et al., 2008; Yang and Proweller, 2011). Blockade of Pdgf signaling leads to insufficient proliferation and recruitment of PCs/vSMCs with associated perinatal lethality; specifically, PdgfBB and Pdgfrβ knockout mice exhibit compromised blood vessel integrity in skin and mesenteric territories as well as disorganization of kidney glomeruli (Lindahl et al., 1997; Stratman et al., 2010). In SM22-Cre^{+}/DNMAML1^{+} embryos, AComA-associated vSMCs were reduced in number and in proliferative capacity compared to controls. Therefore, relatively poor mural investment of cerebral arteries from SM22-Cre^{+}/DNMAML1^{+} embryos is consistent with deficiency of Pdgfrβ and suggests that a Notch-Pdgf axis contributes to proper migration and recruitment of SMC during cW/AComA formation.

Observations and quantitative descriptions of EC behavior and Jagged1 expression in vSMCs

Interestingly, we identified reduced proliferative capacity of ECs associated with AComA formation in SM22-Cre^{+}/DNMAML1^{+} embryos. This finding is reminiscent of our previous report wherein ECs, co-cultured with adult SM22-Cre^{+}/DNMAML1^{+} aortic SMCs deficient in Jagged1, displayed reduced proliferative activity concomitant with decreased EC Notch1 stimulation (Yang and Proweller, 2011). Herein, we demonstrate that despite an existing

Vegfa gradient at the region of AComA assembly, angiogenesis is markedly compromised in SM22-Cre$^+$/DNMAML1$^+$ embryos and suggest that reduced EC proliferation results from non-productive interactions with Notch signaling-defective vSMCs. Specifically, impaired Jagged1 expression in prenatal SM22-Cre$^+$/DNMAML1$^+$ cerebral SMCs may reduce effective engagement with EC Notch receptors necessary for proper AComA angiogenesis. Whether Jagged1 contribution from cerebral SMCs is necessary and sufficient for competent AComA formation requires further investigation. Recent reports of smooth muscle Jagged1-deficient mice have thus far revealed critical abnormalities in liver organogenesis and ductus arteriosus closure resulting in perinatal lethality (Feng et al., 2010; Hofmann et al., 2010). Alternatively, the combined molecular reductions in Pdgfrβ and Jagged1 in SM22-Cre$^+$/DNMAML1$^+$ cerebral vSMCs could underlie the vSMC impairments leading to abnormal cW assembly.

Model for vSMC Notch signaling regulation of AComA assembly

In this first time study in mice, we have anatomically characterized a unique temporospatial developmental process of cW formation during gestation with special attention to the AComA assembly, the clinically important arterial collateral linking bi-hemispheric anterior cerebral circulation (Hoksbergen et al., 2003; Profice et al., 2011). AComA and cW formation, in particular, are exquisitely sensitive to perturbations in smooth muscle Notch signaling, confirming a developmental basis and explanation for corrupt cW anatomy observed in adult SM22-Cre$^+$/DNMAML1$^+$ animals (Yang and Proweller, 2011). Our new data at the developmental level support models in which vSMC migration via the Pdgf signaling axis and engagement of EC Notch receptors by smooth muscle Jagged1 promotes optimal EC angiogenic responses (see model, Fig. 10). The susceptibility of AComA formation with otherwise proper distribution of the major proximal cerebral vessels remains particularly surprising as the loss of vSMC is not limited to the AComA region. Since the AComA is a collateral conduit, it is conceivable that a component of flow-dependent regulation may be contributing in a Notch signaling-dependent manner but this remains to be explored. Though we suggest that reductions in EC proliferation might result from non-productive interaction with existing Notch signaling-defective vSMCs, further molecular studies will be required to dissect the localized mechanisms of angiogenic regulation particularly in anatomical regions (such as AComA) replete with Vegfa. Importantly, our prenatal animal studies provide significant insight into the sensitive and complex regulation of cW formation from a vSMC perspective, offering a new conceptual framework towards understanding human congenital cW anomalies.

Supplementary Material

Refer to Web version on PubMed Central for supplementary material.

Acknowledgments

We thank Dr. Diana Ramirez-Bergeron for sharing equipment, reagents, and helpful comments on the manuscript. We thank Ronald Midura for contrast reagents and Amit Vasanji and Richard J. Rozic (ImageIQ, Cleveland, OH) for assistance with μCT imaging. This work was supported by National Institutes of Health Grant R01-HL096603-01 to A.P.

References

Armulik A, Genove G, Mae M, Nisancioglu MH, Wallgard E, Niaudet C, He L, Norlin J, Lindblom P, Strittmatter K, Johansson BR, Betsholtz C. Pericytes regulate the blood-brain barrier. Nature. 2010; 468:557–61. [PubMed: 20944627]

Barone FC, Knudsen DJ, Nelson AH, Feuerstein GZ, Willette RN. Mouse strain differences in susceptibility to cerebral ischemia are related to cerebral vascular anatomy. J Cereb Blood Flow Metab. 1993; 13:683–92. [PubMed: 8314921]

Bauer HC, Steiner M, Bauer H. Embryonic development of the CNS microvasculature in the mouse: new insights into the structural mechanisms of early angiogenesis. EXS. 1992; 61:64–8. [PubMed: 1377576]

Benedito R, Roca C, Sorensen I, Adams S, Gossler A, Fruttiger M, Adams RH. The notch ligands Dll4 and Jagged1 have opposing effects on angiogenesis. Cell. 2009; 137:1124–35. [PubMed: 19524514]

Bonkowski D, Katyshev V, Balabanov RD, Borisov A, Dore-Duffy P. The CNS microvascular pericyte: pericyte-astrocyte crosstalk in the regulation of tissue survival. Fluids Barriers CNS. 2011; 8:8. [PubMed: 21349156]

Chalothorn D, Faber JE. Formation and maturation of the native cerebral collateral circulation. J Mol Cell Cardiol. 2010; 49:251–9. [PubMed: 20346953]

Etchevers HC, Vincent C, Le Douarin NM, Couly GF. The cephalic neural crest provides pericytes and smooth muscle cells to all blood vessels of the face and forebrain. Development. 2001; 128:1059–68. [PubMed: 11245571]

Feng X, Krebs LT, Gridley T. Patent ductus arteriosus in mice with smooth muscle-specific Jag1 deletion. Development. 2010; 137:4191–9. [PubMed: 21068062]

Fujita M, Cha YR, Pham VN, Sakurai A, Roman BL, Gutkind JS, Weinstein BM. Assembly and patterning of the vascular network of the vertebrate hindbrain. Development. 2011; 138:1705–15. [PubMed: 21429985]

Gerber HP, Dixit V, Ferrara N. Vascular endothelial growth factor induces expression of the antiapoptotic proteins Bcl-2 and A1 in vascular endothelial cells. J Biol Chem. 1998; 273:13313–6. [PubMed: 9582377]

Hiruma T, Nakajima Y, Nakamura H. Development of pharyngeal arch arteries in early mouse embryo. J Anat. 2002; 201:15–29. [PubMed: 12171473]

Hofmann JJ, Zovein AC, Koh H, Radtke F, Weinmaster G, Iruela-Arispe ML. Jagged1 in the portal vein mesenchyme regulates intrahepatic bile duct development: insights into Alagille syndrome. Development. 2010; 137:4061–72. [PubMed: 21062863]

Hoksbergen AW, Legemate DA, Csiba L, Csati G, Siro P, Fulesdi B. Absent collateral function of the circle of Willis as risk factor for ischemic stroke. Cerebrovasc Dis. 2003; 16:191–8. [PubMed: 12865604]

James JM, Gewolb C, Bautch VL. Neurovascular development uses VEGF-A signaling to regulate blood vessel ingression into the neural tube. Development. 2009; 136:833–41. [PubMed: 19176586]

Jin S, Hansson EM, Tikka S, Lanner F, Sahlgren C, Farnebo F, Baumann M, Kalimo H, Lendahl U. Notch signaling regulates platelet-derived growth factor receptor-beta expression in vascular smooth muscle cells. Circ Res. 2008; 102:1483–91. [PubMed: 18483410]

Korn J, Christ B, Kurz H. Neuroectodermal origin of brain pericytes and vascular smooth muscle cells. J Comp Neurol. 2002; 442:78–88. [PubMed: 11754368]

Kurz H. Cell lineages and early patterns of embryonic CNS vascularization. Cell Adh Migr. 2009; 3:205–10. [PubMed: 19270493]

Lackovic V, Kostic V, Sternic N, Kanjuh V, Vukovic I. Angiogenesis in the central nervous system: a role of vascular endothelial growth factor. Vojnosanit Pregl. 2005; 62:59–67. [PubMed: 15715351]

Lindahl P, Johansson BR, Leveen P, Betsholtz C. Pericyte loss and microaneurysm formation in PDGFB-deficient mice. Science. 1997; 277:242–5. [PubMed: 9211853]

Majesky MW. Developmental basis of vascular smooth muscle diversity. Arterioscler Thromb Vasc Biol. 2007; 27:1248–58. [PubMed: 17379839]

Mancuso MR, Kuhnert F, Kuo CJ. Developmental angiogenesis of the central nervous system. Lymphat Res Biol. 2008; 6:173–80. [PubMed: 19093790]

Mason HA, Rakowiecki SM, Gridley T, Fishell G. Loss of notch activity in the developing central nervous system leads to increased cell death. Dev Neurosci. 2006; 28:49–57. [PubMed: 16508303]

Morrow D, Cullen JP, Liu W, Guha S, Sweeney C, Birney YA, Collins N, Walls D, Redmond EM, Cahill PA. Sonic Hedgehog induces Notch target gene expression in vascular smooth muscle cells via VEGF-A. Arterioscler Thromb Vasc Biol. 2009; 29:1112–8. [PubMed: 19407245]

Okuyama S, Okuyama J, Tamatsu Y, Shimada K, Hoshi H, Iwai J. The arterial circle of Willis of the mouse helps to decipher secrets of cerebral vascular accidents in the human. Med Hypotheses. 2004; 63:997–1009. [PubMed: 15504567]

Profice P, Pilato F, Broccolini A, Santoliquido A, Marca GD, Di Lazzaro V. Right hemiparesis in right carotid stenosis. Circulation. 2011; 124:360–2. [PubMed: 21768554]

Proweller A, Wright AC, Horng D, Cheng L, Lu MM, Lepore JJ, Pear WS, Parmacek MS. Notch signaling in vascular smooth muscle cells is required to pattern the cerebral vasculature. Proc Natl Acad Sci U S A. 2007; 104:16275–80. [PubMed: 17909179]

Stratman AN, Schwindt AE, Malotte KM, Davis GE. Endothelial-derived PDGF-BB and HB-EGF coordinately regulate pericyte recruitment during vasculogenic tube assembly and stabilization. Blood. 2010; 116:4720–30. [PubMed: 20739660]

Vasudevan A, Bhide PG. Angiogenesis in the embryonic CNS: a new twist on an old tale. Cell Adh Migr. 2008; 2:167–9. [PubMed: 19262109]

Yang K, Proweller A. Vascular smooth muscle Notch signals regulate endothelial cell sensitivity to angiogenic stimulation. J Biol Chem. 2011; 286:13741–53. [PubMed: 21349836]

Abbreviations

cW	circle of Willis
ACA	anterior cerebral artery
AComA	anterior communicating artery
OA	ophthalmic artery
BA	basilar artery
ICA	internal carotid artery
MCA	middle cerebral artery
PCA	posterior cerebral artery
PComA	posterior communicating artery
Vegfa	vascular endothelial growth factor-a
Vegfr-2	vascular endothelial growth factor receptor-2
Pdgf	platelet derived growth factor-bb
Pdgfrp	platelet derived growth factor receptor beta
vSMC	vascular smooth muscle cell
PC	pericyte

Highlights

- The circle of Willis (cW) is an angiogenically derived cerebral arterial structure.
- cW assembly is developmentally regulated by smooth muscle Notch signaling.
- Notch-dependent cW abnormalities in mice show similarity to human cW variants.
- Vascular smooth muscle Notch signaling modulates endothelial cell proliferation.
- Vascular smooth muscle exhibits a key role in regulating cerebral angiogenesis.

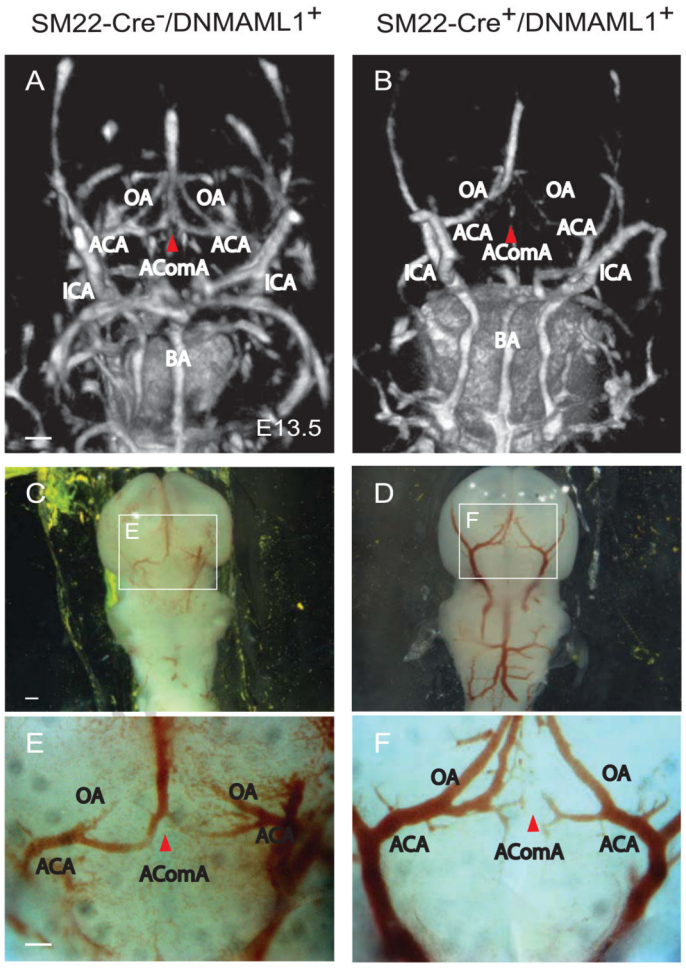

Fig. 1. μ-CT and bright field imaging reveals abnormal patterning of the cW/AComA in SM22-Cre^{+}/DNMAML1^{+}embryos

(A, B) μ-CT and (C-F) bright field imaging of proximal cerebral arteries at E13.5 (ventral view). Boxed regions in C and D are shown at higher magnification in E and F, respectively. In control SM22-Cre^{-}/DNMAML1^{+} embryos, formation of major cerebral arteries including ICA and BA is complete. The AComA segment at the anterior portion of the cW is symmetrically united by branches from left and right ACAs (A, E, red arrowhead). In contrast, there is notable absence of AComA segment opacification and incomplete anastomoses in SM22-Cre^{+}/DNMAML1^{+} embryos (B, F, red arrowheads). N=3 per group/imaging modality. Scale bars: 20 μm (A, B and C, F) or 50 μm (C, D). ICA, internal carotid artery; BA, basilar artery; OA, olfactory artery; AComA, anterior communicating artery; ACA, anterior cerebral artery.

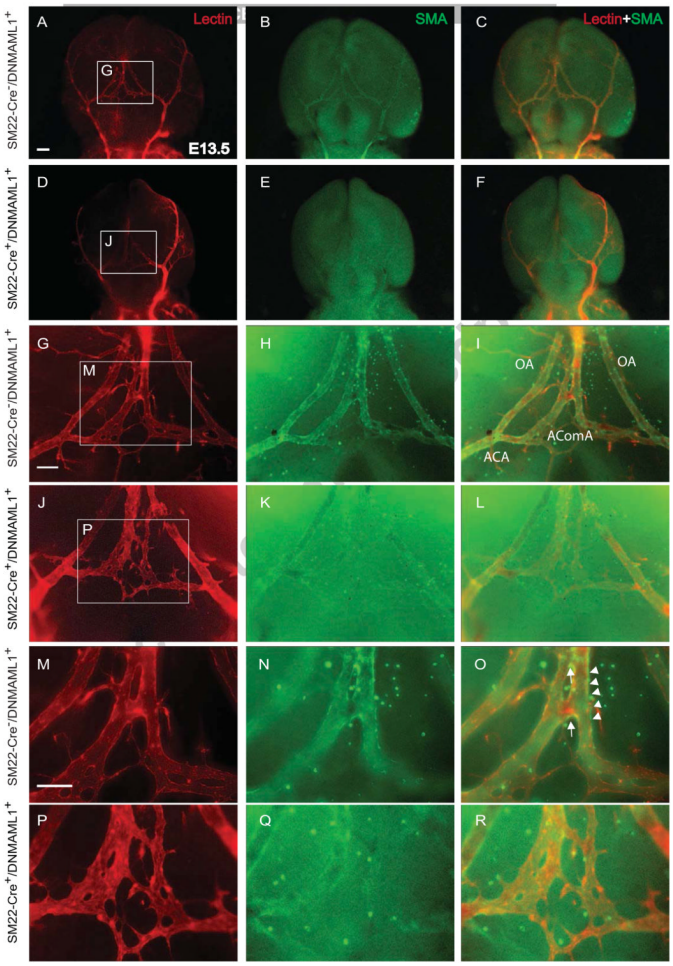

Fig. 2. Notch signaling-deficient embryos exhibit delayed vascular plexus formation of the AComA

(A-F) Ventral view of cerebral arteries from control and mutant SM22-Cre^{+}/DNMAML1^{+} embryos at E13.5 perfused with lectin (red, ECs) and whole mount immunostained with FITC-anti-SMA antibody (green, vSMCs). Merged images reflect the fluorescent overlay of lectin-SMA double labeling. Boxed regions in A, D, G and J are shown at higher magnification in panels G, J, M and P, respectively. Within the anterior portion of the cW, the lectin-stained vascular network is delayed and poorly remodeled with few SMCs in SM22-Cre^{+}/DNMAML1^{+} embryos (K, L and Q, R) in contrast to discrete tubular, remodeled segments in controls (H, I and N, O, arrowheads). Note that the anastomoses of the future AComA in control embryos shows extensive vSMC coverage (O, arrow), otherwise absent in the mutant (R). N=3 per group. Scale bars: 50 μm (A–F) or 10 μm (G-R). OA, olfactory artery; AComA, anterior communicating artery; ACA, anterior cerebral artery.

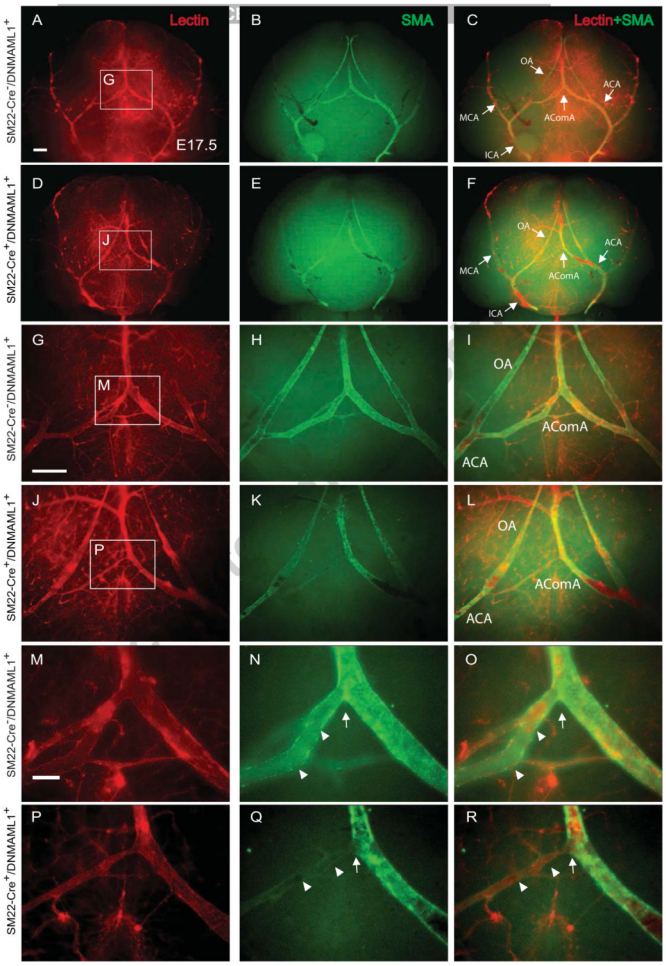

Fig. 3. Malformation of the cW with underdeveloped AComA in SM22-Cre^{+}/DNMAML1^{+}embryos

(A-F) Proximal cerebral arterial vasculature at the ventral surface of dissected brains in E17.5 control and SM22-Cre^{+}/DNMAML1^{+} embryos is identified by EC-specific lectin labeling (red) and whole mount smooth muscle cell actin (SMA, green) staining in low magnification. Merged images show the fluorescent overlay of lectin and SMA double labeling. Panels G-L and M-R are magnified from representative boxed regions of upper panels. Mature AComAs in control embryos display uniform vessel calibers and symmetry with continuous SMC alignment along lectin-lined segments (N and O, arrowheads) and at the convergence point formed by bilateral branches of the ACAs (O, arrow). In contrast, SM22-Cre^{+}/DNMAML1^{+} embryos typically exhibit diminished and discontinuous SMC alignment along existing unilateral branches of ACA (Q and R, arrowheads) as well as at the AComA connection site (R, arrow). N=3 per group. Scale bars: 50 μm (A–I) and 10 μm (M-R). MCA, middle cerebral artery, ICA, internal carotid artery; BA, basilar artery; OA, olfactory artery; AComA, anterior communicating artery; ACA, anterior cerebral artery.

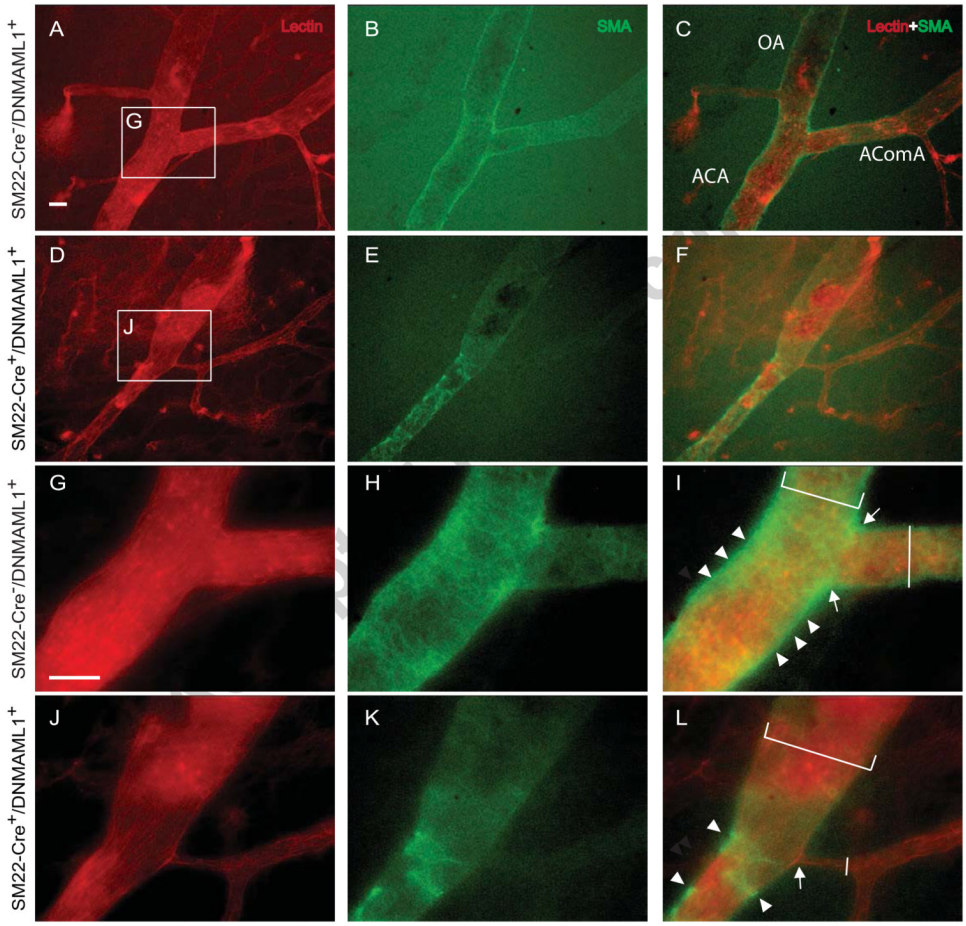

Fig. 4. SM22-Cre^{+}/DNMAML1^{+}embryos display dilated OA and ACA vessels lacking SMC coverage

(A-L) EC-specific lectin (red) and smooth muscle actin (SMA, green) staining identifies SMC coverage at regions of ACA bifurcation (AComA and OA) in E17.5 embryos. Unlike enrichment of SMCs (arrowheads) at branch points (arrow) of ACAs in control embryos (G-I), SMCs are poorly detected (arrowheads) at the branch points (arrow) of mutant ACAs (J-L, arrow). Mutant OAs also display dilated vessel calibers with diminished SMC coverage (K, L, white bracket) in contrast to the uniform calibers and smooth muscle coated OA from controls (H, I, white bracket). Moreover, typically observed unilateral AComAs in SM22-Cre^{+}/DNMAML1^{+} embryos exhibit reduced SMC coverage with abnormal caliber (L, vertical white line) in contrast to the remodeled AComAs in controls (I, vertical white line). Panels G-L are magnifications of representative boxed regions in upper panels. N=3 per group. Scale bar: 5 μm. OA, olfactory artery; AComA, anterior communicating artery; ACA, anterior cerebral artery.

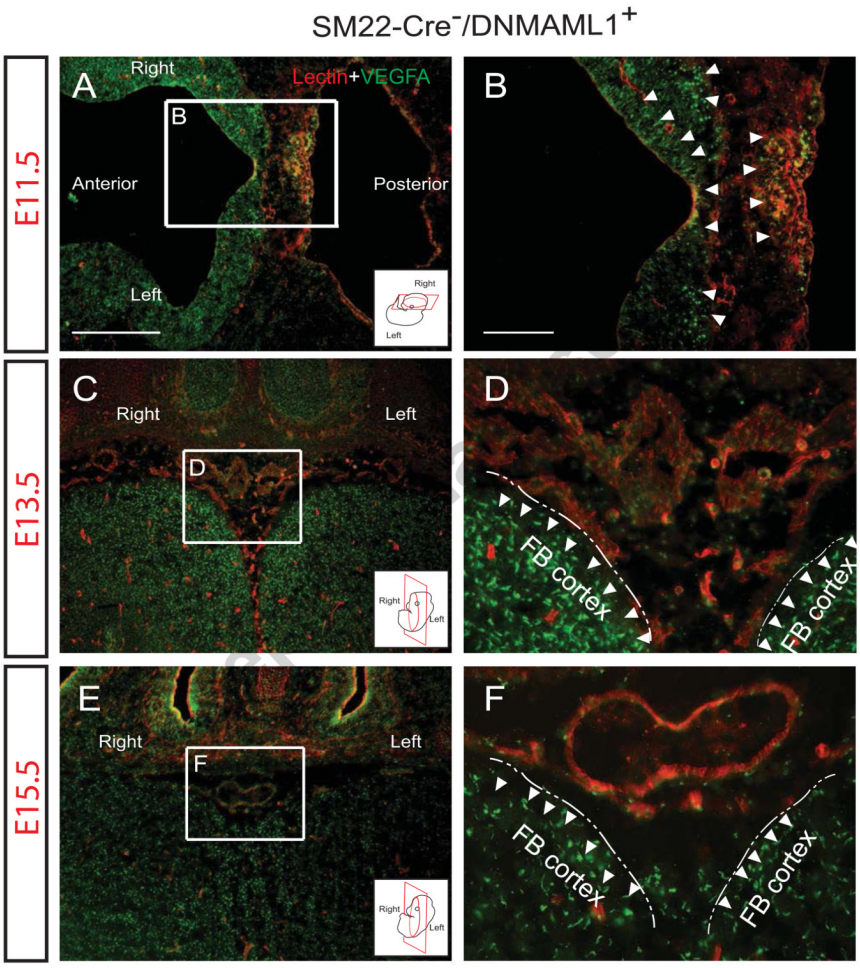

Fig. 5. EC plexus growth of AComA occurs in the presence of Vegfa

Vegfa detection (green) in representative sections of E11.5 (A, B, transverse), E13.5 (C, D, coronal) and E15.5 (E, F, coronal) control embryonic brains at the level of the optic chiasm (cartoon inserts display orientation). Panels B, D and F are magnified from boxed regions in A, C and E, respectively. (A, B) Vegfa is expressed in the neural tube (arrowheads) of forebrain and hindbrain, encompassing regions of lectin-labeled (red) EC plexus. Lectin-labeled lumen structures adjacent to Vegfa-concentrated neuronal tissue (arrowheads) were observed at AComA regions of both E13.5 (C, D) and E15.5 embryos (E, F). Note that bilateral EC segments of AComA merge to form a single lumen vessel in E15.5 embryos (F). Dash lines in D and F define the boundary of bilateral forebrain (FB) cortex. N =3). Scale bars: 50 μm (A, C and E) and 10 μm (B, D and F).

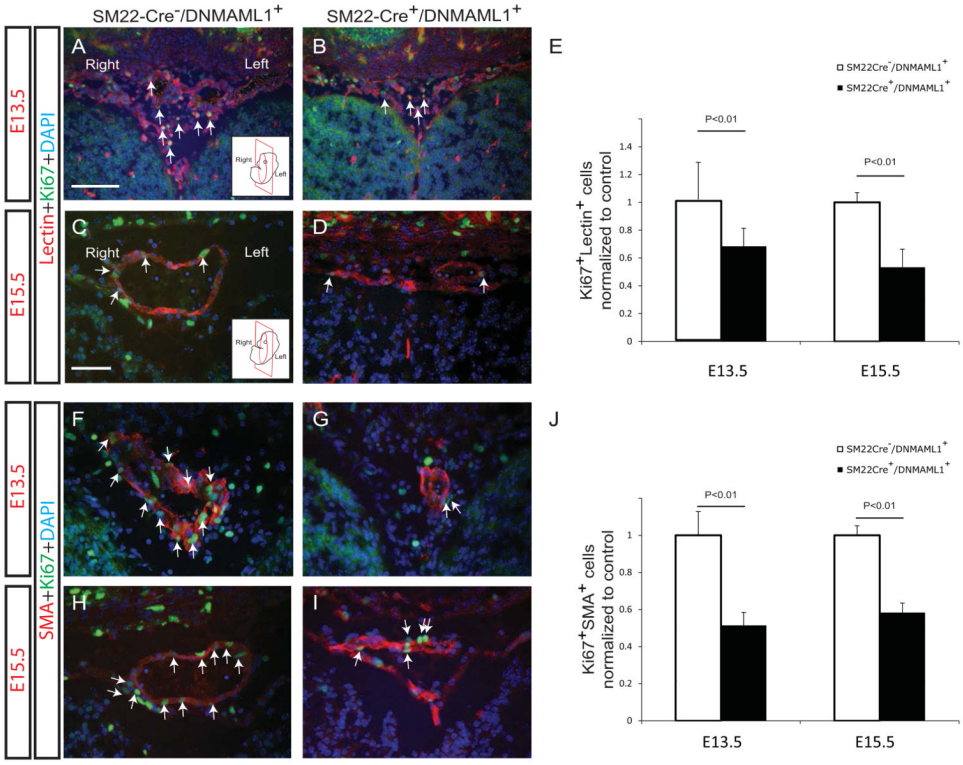

Fig. 6. SM22-Cre^{+}/DNMAML1^{+}embryos exhibit impaired EC and vSMC proliferation in AComA region

Double-staining of proliferation marker Ki67 with either lectin (A-D) or SMA (F-I) in representative coronal sections from E13.5 and E15.5 embryos reveals altered EC and vSMC proliferation associated with mutant AComA assembly. Ki67^{+}Lectin^{+} cells (A-D, arrows) or Ki67^{+}SMA^{+} cells (F-I, arrows) are abundant in association with developing AComA plexus in controls (A, C, F and H) in the contrast to SM22-Cre^{+}/DNMAML1^{+}embryos (B, D, G and I). Nuclei identified by DAPI counterstain (blue). Quantification of Ki67^{+}Lectin^{+} (E) or Ki67^{+}SMA^{+} (J) cells in AComA assembly region. Data represent mean±SEM percentage of cell numbers per high power field normalized to controls (N=6 sections per embryo, N=3 embryos per stage, p<0.01). Cartoon inserts in A and C represent coronal orientation. Scale bars: 50 μm (A and B) and 10 μm (C- I).

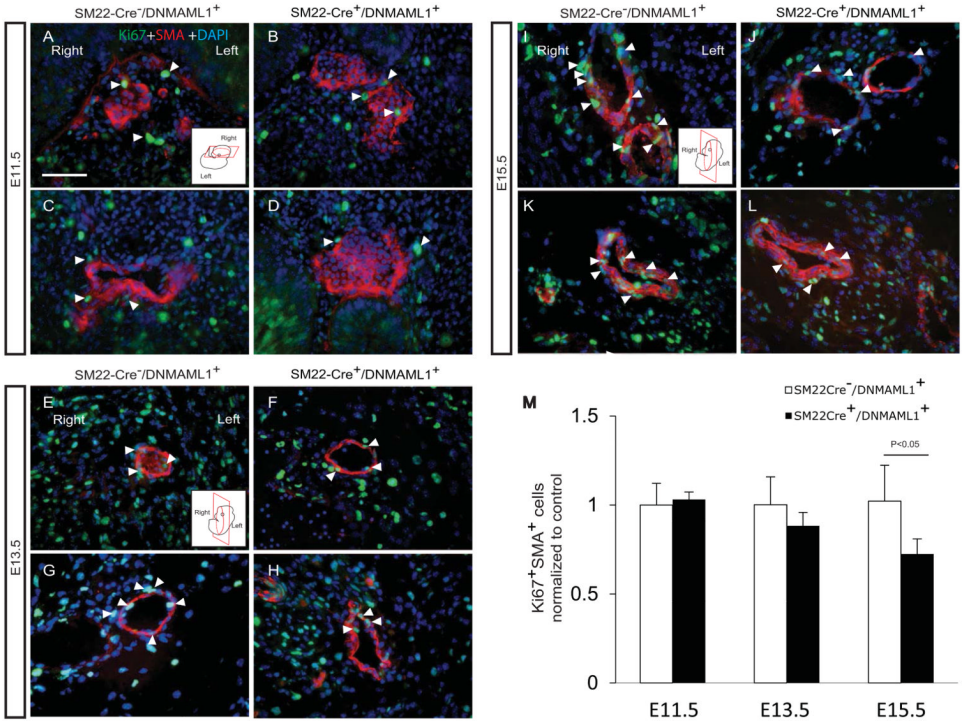

Fig. 7. Impaired vSMC proliferation in proximal cerebral arteries from SM22-Cre$^+$/ DNMAML1$^+$embryos

Ki67$^+$SMA$^+$ double-staining identifies proliferating vSMCs in olfactory (A-B, E-F, I-J) and middle cerebral (C-D, G-H, K-L) arteries from control and SM22-Cre$^+$/ DNMAML1$^+$embryonic brains at the indicated stages. Cartoon inserts in A, E and I represent section orientation for each stage. At E11.5, comparable numbers of proliferating vSMCs are observed in control (A, C) and mutant (B, D) embryos. However, reduced SMC proliferation (yellow, arrowheads) is observed in mutants beginning E13.5 (F-G), achieving statistical significance by E15.5 (J-L). Nuclei identified by DAPI counterstain (blue). (M) Quantification of Ki67$^+$SMA$^+$ cell numbers from controls and mutants at indicated stages. Data represent mean±SEM percentage of cell numbers per high power field normalized to controls (N=6 sections per embryo, N=3 embryos per stage, p<0.05 at E15.5). Scale bars: 10 μm.

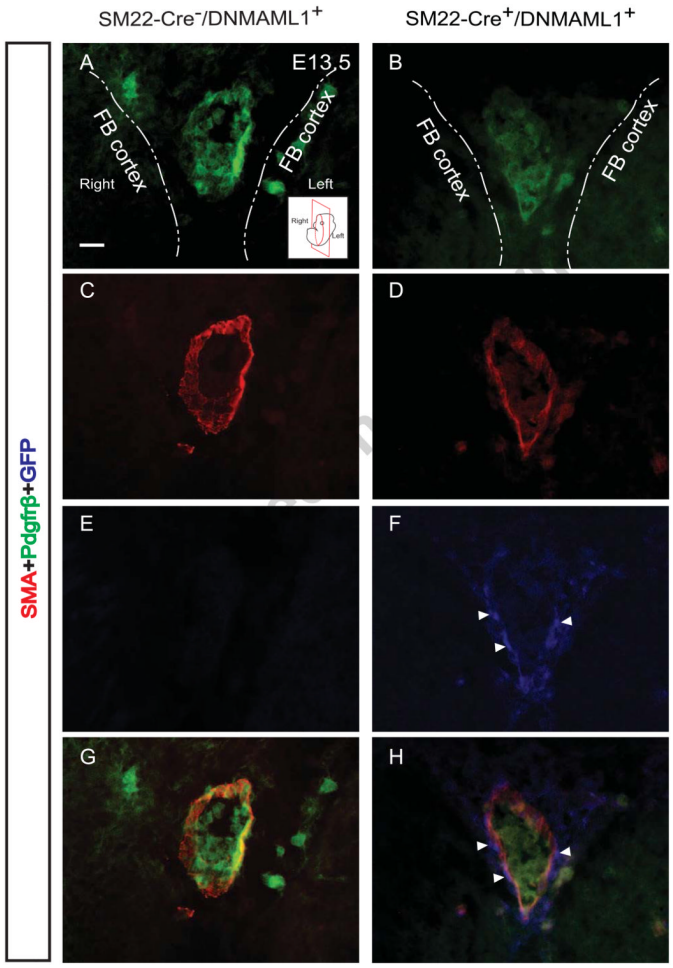

Fig. 8. Attenuated Pdgfrp expression in SM22-Cre^{+}/DNMAML1^{+}vSMCs during AComA assembly

Immunohistochemical analyses of E13.5 control embryos reveal enriched Pdgfrβ^{+}/SMA^{+}/GFP- (A, C, E, G) SMCs along the merged AComA/ACA conduit segment of the cW. In contrast, corresponding SM22-Cre^{+}/DNMAML1^{+} vessel segments display reduced Pdgfrβ within existing DNMAML1^{+} (GFP^{+})/SMA^{+} SMCs (B, D, F, H). Arrowheads indicate nuclear localization of DNMAML1 (GFP^{+}). Dash lines in each panel define the boundary of bilateral forebrain (FB) cortex. Note stain color: Pdgfrβ^{+} (green), SMA^{+} (red), GFP^{+} (blue). A representative cartoon insert (A) illustrates the coronal section plane near level of the optic chiasm. N=3 per group. Scale bars: 10 μm.

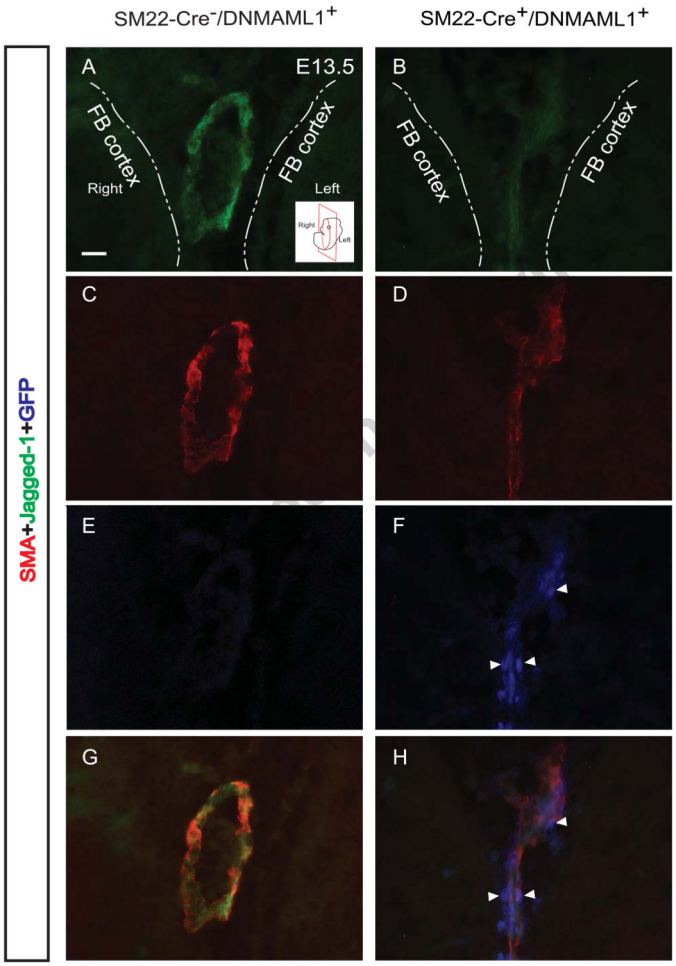

Fig. 9. Jagged1 content is reduced in SM22-Cre^{+}/DNMAML1^{+}vSMCs associated with cW/AComA assembly

Similar to panel sections in Fig. 8, immunohistochemical analyses of E13.5 control embryos reveal abundant Jagged1^{+}/SMA^{+}/GFP- (A, C, E, G) SMCs of the thin tunica media in merged AComA/ACA conduit segments. In contrast, corresponding SM22-Cre^{+}/DNMAML1^{+} vessel segments display markedly reduced Jagged1 expression within existing DNMAML1^{+} (GFP^{+})/SMA^{+} SMCs (B, D, F, H). Arrowheads indicate nuclear localization of DNMAML1 (GFP^{+}). Note stain color: Jaggedl^{+} (green), SMA^{+} (red), GFP^{+} (blue). Dash lines in each panel define the boundary of bilateral forebrain (FB) cortex. A representative cartoon insert (A) illustrates the coronal section plane near level of the optic chiasm. N=3 per group. Scale bars: 10 μm.

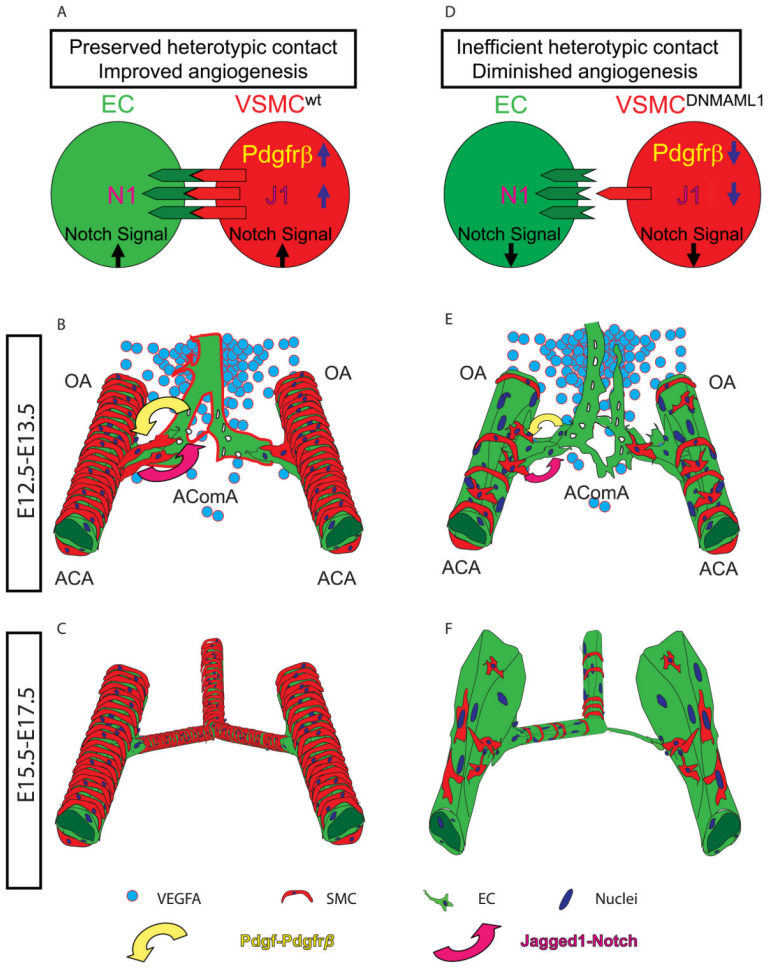

Fig. 10. Model of vSMC Notch signaling contribution to prenatal AComA assembly

(A) In wild-type vSMCs, Notch signaling promotes endogenous expression of Pdgfrβ and Jagged1, permitting optimal association with, and stimulation of, neighboring EC Notch receptors. (B) At mid-gestation (E12.5-13.5), substantial mural coverage indicative of vascular remodeling of the proximal ACAs promotes interaction between SMCs and ECs through ligand engagement of EC Notch receptors, sensitizing ECs to local angiogenic cues such as a graded Vegf signal (blue circles) resulting in early AComA plexus formation. (C) During late gestation (E15.5-17.5), a mature AComA anastomosis is present and characterized by uniform mural coverage and caliber. (D) Notch signaling-deficient vSMCs (i.e. DNMAML1-expressing) feature (1) reduced Pdgfrβ content leading to insufficient proliferation and recruitment of SMCs along the ACA and OA segments and (2) reduced Jagged1 levels collectively resulting in inefficient heterotypic contact with ECs. This results in diminished EC Notch activation and angiogenic sensitivity to available Vegf and a failure of early AComA plexus formation (E). (F) By late gestation, SM22-Cre^{+}/DNMAML1^{+} embryos display an incomplete AComA anastomosis with non-uniform calibers and asymmetric branching at bifurcations of ACAs. OA, olfactory artery; AComA, anterior communicating artery; ACA, anterior cerebral artery.